FOLIA HISTOCHEMICA ET CYTOBIOLOGICA
Vol. 62, No. 1, 2024
pp. 13–24

ORIGINAL PAPER

VIA MEDICA

Nephroprotective effect of Ginsenoside Rg1 in lipopolysaccharide-induced sepsis in mice through the SIRT1/NF-κB signaling

Yadan Hu[1*], Chao Xiang[2*], Dong Zhang[1], Fang Zhou[1], Dede Zhang[1]

[1]Emergency Department, Wuhan Hospital of Traditional Chinese Medicine, Wuhan, China
[2]Massage Department, Wuhan Hospital of Traditional Chinese Medicine, Wuhan, China
*These authors contributed equally to this work.

Abstract

Introduction. During sepsis, the kidney is one of the most vulnerable organs. Sepsis-associated acute kidney injury (S-AKI) is hallmarked by renal inflammation, apoptosis, and oxidative injury. Ginsenoside Rg1 (Rg1) is a natural product that possesses abundant pharmacological actions and protects against many sepsis-related diseases. Nevertheless, its role and related mechanism in S-AKI remain to be determined.

Materials and methods. S-AKI was induced using lipopolysaccharide (LPS, 10 mg/kg) *via* a single intraperitoneal injection. Rg1 (200 mg/kg) was intraperitoneally administered for 3 consecutive days before LPS treatment. For histopathological examination, murine kidney tissues were stained with hematoxylin and eosin. Tubular injury score was calculated to evaluate kidney injury. Serum creatinine and BUN levels were measured for assessing renal dysfunction. The levels and activities of oxidative stress markers (MDA, 4-HNE, PC, GSH, SOD, and CAT) in renal tissue were measured by corresponding kits. Renal cell apoptosis was detected by TUNEL staining. The protein levels of apoptosis-related markers (Bcl-2, Bax, and Cleaved caspase-3), proinflammatory factors, SIRT1, IκBα, p-NF-κB p65, and NF-κB p65 in kidneys were determined using western blotting. Immunofluorescence staining was employed to assess p-NF-κB p65 expression in renal tissues.

Results. LPS-induced injury of kidneys and renal dysfunction in mice were ameliorated by Rg1. Rg1 also impeded LPS-evoked renal cell apoptosis in kidneys. Moreover, Rg1 attenuated LPS-triggered inflammation and oxidative stress in kidneys by inhibiting proinflammatory cytokine release, enhancing antioxidant levels and activities, and reducing lipid peroxidation. However, all these protective effects of Rg1 in LPS-induced AKI mice were reversed by EX527, an inhibitor of sirtuin 1 (SIRT1). Mechanistically, Rg1 upregulated SIRT1 protein expression, increased SIRT1 activity, and inactivated NF-κB signaling in the kidney of LPS-induced AKI mice, which was also reversed by EX527.

Conclusions. Rg1 ameliorates LPS-induced kidney injury and suppresses renal inflammation, apoptosis, and oxidative stress in mice *via* regulating the SIRT1/NF-κB signaling. *(Folia Histochemica et Cytobiologica 2024, Vol. 62, No. 1, 13–24)*

Keywords: mouse; LPS; acute kidney injury; Ginsenoside Rg1; sirtuin 1; NF-κB; oxidative stress; apoptosis

Introduction

Sepsis refers to a life-threatening inflammatory disorder caused by abnormal response to bacterial infection and is the main cause of acute kidney injury (AKI), accounting for about 50% of AKI cases in intensive care units [1]. Sepsis-associated AKI (S-AKI) is a renal disease with extremely high mortality, characterized by serious kidney disfunction and renal cell death [2]. The pathophysiology of S-AKI is complex, which has yet not been elucidated completely [3]. Although efforts have been made to investigate new therapeutic strategies in recent years, no specific and effective therapies for the treatment of S-AKI are determined currently [4]. Hence, it is necessary to figure out

Correspondence address:
Dede Zhang
Wuhan Hospital of Traditional Chinese Medicine, No.303 Sixin Avenue, Hanyang District, Wuhan, China
e-mail: Zddd1991@hotmail.com

Folia Histochem Cytobiol. 2024
DOI: 10.5603/fhc.97140
ISSN 0239-8508, e-ISSN 1897-5631

www.journals.viamedica.pl/folia_histochemica_cytobiologica

underlying pathogenic mechanisms and search for novel therapeutic approaches to improve the clinical outcomes of patients with S-AKI.

Kidney inflammation and oxidative stress are key contributing factors in S-AKI [5]. Lipopolysaccharide (LPS), an endotoxin, is an important component of Gram-negative bacteria and is widely utilized to establish S-AKI models [6]. Under LPS stimulation, the ROS release is excessive and antioxidative enzyme system is disrupted in the kidney, which leads to aggravation of renal oxidative stress [7]. Moreover, proinflammatory cytokine production is increased after LPS challenge in the kidney, thereby inducing inflammatory response [8]. The oxidative injury and inflammation under LPS stimulation also contribute to mitochondrial dysfunction and renal cell apoptosis, ultimately facilitating S-AKI pathogenesis [7, 9]. Therefore, finding preventive measures that can control renal oxidative stress and inflammation may be an available strategy for S-AKI treatment.

Ginsenoside Rg1 (Rg1) is one of the active compounds extracted from the root of *Panax ginseng* and it possesses multiple pharmacological properties, such as immunoregulatory, anti-inflammatory, antioxidant and anti-apoptotic as well as neuroprotective and cardioprotective activities [10]. Numerous studies have illuminated the beneficial role of Rg1 in sepsis and sepsis-related disorders. For example, in the mouse model of polymicrobial sepsis, Rg1 enhances innate immunity and restrains inflammation and apoptosis of lymphocytes to improve survival of mice [11]. Rg1 protects against sepsis-associated encephalopathy by increasing antioxidant enzyme activities, reducing proinflammatory cytokine release, and inhibiting neuronal apoptosis [12]. Rg1 attenuates cardiomyocyte injury and improves cardiac function in mice with septic myocardial dysfunction through its anti-apoptotic and anti-inflammatory properties [13]. Notably, accumulating reports have disclosed that Rg1 attenuates podocyte injury induced by angiotensin II [14], experimental glomerular nephritis [15], and glomerular fibrosis [16]. However, the nephroprotective role of Rg1 in S-AKI has yet not been reported.

Silent information regulator Sirtuin 1 (SIRT1) is a NAD^+-dependent histone deacetylase that participates in the regulation of many physiological and pathophysiological processes including oxidant stress and inflammation [17]. Accumulating evidence has proven that the upregulation of SIRT1 acts protective against S-AKI [18, 19]. Moreover, SIRT1 is closely related to the inactivation of NF-κB inflammatory pathway [20]. Activated NF-κB boosts excessive release of proinflammatory factors in many inflammation and sepsis models [21]. Previously, Lu *et al.*[22] noted that quercetin nanoparticles mitigate renal dysfunction, renal inflammation, and apoptosis in LPS-induced S-AKI experimental models by regulating SIRT1/ /NF-κB signaling. Wang *et al.* [23] reported that Rg1 prevents lung injury induced by sepsis by relieving pulmonary inflammation and endoplasmic reticulum stress through the regulation of SIRT1. However, whether Rg1 can regulate SIRT1/NF-κB signaling pathways in S-AKI remains unclear.

In our current investigation, we focused on the biological function and the mechanism of Rg1 action in LPS-induced S-AKI mice. We hypothesized that Rg1 attenuates LPS-triggered kidney injury through its anti-inflammatory, anti-apoptotic and antioxidant efficacies by regulating SIRT1/NF-κB signaling pathways. This report may lay a theoretical basis for S-AKI treatment.

Materials and methods

Animals and grouping. Forty healthy C57BL/6 mice (male, 8–10 weeks of age; 25–27 g; Japan SLC, Hamamatsu, Japan) were housed at 25 ± 2°C with 50–65% humidity under a cycle of 12-h light/12-h dark. All mice had free access to food and water. Experimental protocols were granted approval from the Ethics Committee of the Graduate School of Medicine at Wuhan Hospital of Traditional Chinese Medicine. AKI was induced using LPS (a dose of 10 mg/kg, dissolved in 0.9% NaCl) *via* a single intraperitoneal injection (*i.p.*) as described by Nadeem *et al.* [24]. All mice were assigned into four groups (n = 10 *per* group) and received treatment as follows: 1. Control group: mice were treated with the vehicle (1 mL 0.9% NaCl, *i.p.*). 2. LPS group: mice received a single dose of LPS (10 mg/kg, *i.p.*). 3. LPS + Rg1 group: mice received Rg1 (200 mg/kg/d, dissolved in 0.9% NaCl, *i.p.*) for 3 consecutive days prior to LPS treatment. 4. LPS + ISO + EX527: mice received Rg1 (200 mg/ /kg/d, dissolved in 0.9% NaCl, *i.p.* for 3 consecutive days prior to LPS injection) and EX527, a SIRT1 inhibitor (10 mg/kg/d, dissolved in 0.9% NaCl, *i.p.* 30 min prior to Rg1 injection) and then received LPS (10 mg/kg, *i.p.*). The doses of Rg1 and EX527 used in this study were based on the previous studies [25, 26]. Twenty-four hours after LPS treatment, mice were anesthetized for blood sample collection from the ophthalmic artery. All mice were sacrificed *via* CO_2 inhalation followed by cervical dislocation. Both kidneys were collected. Serum samples were kept frozen at –80°C until analyzed. The kidneys were divided into four parts. A quarter of the kidneys were preserved in 10% phosphate-buffered formalin for histological examination. A quarter of the kidneys were used for apoptosis evaluation and immunofluorescence staining. A quarter of the kidneys were used for measurement of the content of inflammatory cytokines and oxidative stress-related markers. A quarter of the kidneys were used for western blotting analysis.

Folia Histochem Cytobiol. 2024
DOI: 10.5603/fhc.97140
ISSN 0239-8508, e-ISSN 1897-5631

Hematoxylin and eosin (HE) staining. After the mice were sacrificed, the renal tissues of different groups were resected and fixed in 4% paraformaldehyde. The fixed tissues were embedded in paraffin, and sectioned (4 μm thick) for dewaxing and dehydration. Tissue sections were then stained with hematoxylin and eosin following standard procedures, dehydrated with ethanol, cleared with xylene and mounted in neutral balsam. The histomorphological changes of the samples was observed employing a light microscope (BX53, Olympus, Tokyo, Japan). As published earlier [27], the kidney injury score was quantified based on the examination results of HE staining. The kidney injury, including tubular enlargement, tubular necrosis, erosion of brush border, cast formation, and vacuolar deterioration, was evaluated by a trained histopathologist blinded to the treatment groups on a scale of 0–5 where 0, 1, 2, 3, 4, and 5 specify 0%, 1–10%, 11–25%, 26–50%, 51–75%, and 76–100% renal injury, respectively.

Western blotting. A quarter of the kidneys were lysed by RIPA buffer (Thermo Fisher Scientific, Waltham, MA, USA), and the protein concentrations were tested by BCA kit (Beyotime, Shanghai, China). Proteins were isolated by 10% SDS–PAGE and transferred onto PVDF membranes (Millipore, Billerica, MA, USA), which were then blockaded by 5% skim milk. After that, membranes were incubated with primary antibodies at 4°C overnight. Then, membranes were rinsed with TBST and incubated with the secondary antibody (1 : 2000, ab6789, Abcam, Cambridge, MA, USA) for 2 h. The membranes were visualized by ECL luminescent liquid (Advansta, Menlo Park, CA, USA). The relative density of protein bands was analyzed by ImageJ (v1.8.0; National Institutes of Health). The primary antibodies used are as follow: SIRT1 [1 : 1000, #2493, Cell Signaling Technology (CST), USA], phospho-p38 MAPK (1 : 1000, #4511, CST), JNK (1 : 1000, #9252, CST), phospho- Bcl-2 (1 : 1000, #15071, CST), Bax (1 : 1000, #14796, CST), Cleaved caspase-3 (1 : 1000, #9661, CST), IκBα (1 : 1000, #4812, CST), NF-κB p65 (1 : 1000, #8242, CST), NF-κB phospho-p65 (1 : 1000, #3033, CST), GAPDH (1 : 1000, #5174, CST), IL-6 (1 : 1000, #12912, CST), IL-1β (1 : 1000, #12703, CST), TNF-α (1 : 1000, #11948, CST). GAPDH served as loading control.

Enzyme-linked immune-sorbent assay (ELISA). Kidney tissues were homogenized in 0.3 g/mL (wet mass) precooled 0.9% NaCl by a high-speed homogenizer (Heidolph, DIAX 900, Heidolph Instruments, Kelheim, Germany) five times for 10 sec at 10,000 × *g*. Following homogenization, the homogenates were subjected to centrifugation at 12,000 × *g* for 10 min at 4°C. The concentrations of IL-1β, IL-6, and TNF-α in the supernatant were estimated by utilizing corresponding ELISA kits (EK-Bioscience, Guangzhou, China) in accordance with suppliers' suggestions.

Measurement of serum indices of renal function. The blood samples were subjected to centrifugation at 2,800 × *g* for 15 min at 4°C to obtain the serum. Based on the manufacturer's instruction, the serum levels of blood urea nitrogen (BUN) and creatinine were assessed *via* corresponding commercial kits (Saipei Biotechology Co., Ltd, Wuhan, China).

Detection of lipid peroxidative and antioxidant markers. Kidney tissues were homogenized in 0.3 g/mL (wet mass w/v) precooled 0.9% NaCl by a high-speed homogenizer (Heidolph, DIAX 900, Heidolph Instruments) five times for 10 sec at 10,000 × *g*. Following homogenization, the homogenates were subjected to centrifugation at 12000 × *g* for 10 min at 4°C. The supernatant was obtained to measure the activities of superoxide dismutase 1 (SOD-1) and catalase (CAT), and the contents of reduced glutathione (GSH) in accordance with instruction of the kits' manufacturer's (Jiancheng Bioengineering Institute, Nanjing, Jiangsu, China). To assess lipid peroxidation, the contents of protein carbonyl groups (PC), 4-hydroxynonenal (4-HNE), and malondialdehyde (MDA) in the supernatant were estimated by specific kits (Bio-diagnostic Co., Giza, Egypt) according to the suppliers' instructions. MDA and PC are expressed as nanomoles *per* gram tissue. 4-HNE is expressed as microgram *per* milliliter. GSH is expressed as microgram *per* gram tissue. SOD and CAT are expressed as micromoles/min/mg (U/mg).

SIRT1 deacetylase activity. The SIRT1 Activity Assay Kit (Fluorometric; ab156065, Abcam) was used to detect SIRT1 activity in the kidney homogenates by measuring the absorbance at 460 nm on a microplate reader (2030 ARVO; PerkinElmer LifeSciences, Boston, MA, USA) according to the manufacturer's instructions.

TdT-mediated dUTP nick end labeling (TUNEL) staining. To detect apoptosis in renal tissue sections, a TUNEL kit (Roche Applied Science, Penzberg, Germany) was used in accordance with the supplier's instruction. Briefly, the paraffin-embedded kidney tissue sections were dewaxed, washed with xylene, rehydrated, and washed with phosphate-buffered saline (PBS) three times. Then, the sections were treated with cell permeability solution for 8 min and 500 μL TUNEL reaction mixture (50 μL TdT and 450 μL fluorescein-labeled dUTP) for 1 h at 37°C in the darkness. Next, the sections were counterstained with 10 μg/ /mL of DAPI for 5 min at room temperature and mounted with a mixture of glycerol and PBS (2:1) under glass coverslip. Finally, five high-power microscope fields were randomly selected from each glass slide to count the number of TUNEL-positive cells under an inverted fluorescence microscope (CKX53; Olympus, Tokyo, Japan). The percentage of TUNEL-positive cells was represented as the apoptosis index [28].

Immunofluorescence staining. The paraffin-embedded renal sections were preprocessed with 10% donkey serum and 0.3% triton X-100. Then sections were incubated at 4°C overnight with primary antibodies against NF-κB phospho-p65 (1 : 100, Abcam). After washing with TBS 3× 10 min, the sections were incubated with appropriate secondary antibodies for 3 h at room temperature. Subsequently, the sections were washed with TBS and stained with Glycerol Mounting Medium (Abcam) that contained DAPI and DABCO. The fluorescence microscope (CKX53; Olympus) was utilized for capturing the images. The

Folia Histochem Cytobiol. 2024
DOI: 10.5603/fhc.97140
ISSN 0239-8508, e-ISSN 1897-5631

number of NF-κB phospho-p65-positive cells *per* tissue section was counted by ImageJ software [29].

Statistical analysis. SPSS 18.0 software (SPSS Inc., Chicago, IL, USA) was used for the statistical analyses. Experimental data obtained from at least triplicate trails was displayed as the mean ± standard error of the mean (SEM). Differences between groups were tested using independent sample *t*-test and multigroup comparisons were achieved *via* one-way analysis of variance, followed by Tukey's *post hoc* test. P-value less than 0.05 was set as the threshold for statistical significance.

Results

Rg1 attenuates LPS-induced renal injury of mice by upregulating SIRT1

To confirm the renal protection afforded by Rg1 in LPS-induced AKI mouse model, HE staining of kidney specimen of indicated groups was conducted. The results of histopathological examination demonstrated that the control rats displayed normal renal structure. Characteristic pathological changes in renal tissues were observed after LPS treatment, manifested as tubular dilation, tubular vacuolization, inflammatory cell infiltration, and severe glomerular wrinkling (Fig. 1A). Conversely, all these renal lesions induced by LPS were attenuated by Rg1 treatment (Fig. 1A).

Subsequently, we probed into whether SIRT1 is involved in Rg1-mediated renal protection in LPS-induced AKI mouse model. Thirty minutes before Rg1 injection, mice received EX527, a SIRT1 inhibitor. As a result, the renal lesions were aggravated in the LPS + Rg1 + EX527 group compared to the LPS+ + Rg1 group (Fig. 1A), suggesting that blockade of SIRT1 offsets protective effect of Rg1 against LPS-elicited renal injury. Additionally, the tubular injury score in the LPS group was significantly higher than that in the Control group, while this increase was antagonized by Rg1 (Fig. 1B). The LPS + Rg1+ + EX527 group exhibited higher tubular injury score than the LPS + + Rg1 group (Fig. 1B). Additionally, parameters related to renal function were also evaluated. As shown in Fig. 1C, D, Rg1 notably suppressed LPS-induced increase in serum creatinine and BUN, whereas EX527 reversed this protective effect. Thus, declined renal function induced by LPS was alleviated by Rg1 but this effect was reversed by EX527 pre-treatment. Overall, Ginsenoside Rg1 mitigates LPS-induced renal injury and renal dysfunction, which is reversed by SIRT1 inhibition.

Rg1 inhibits LPS-triggered renal oxidative stress by upregulating SIRT1

To verify the antioxidative action of Rg1 in LPS-induced AKI murine model, the contents of molecules related to lipid peroxidation (MDA, 4-HNE, and PC), the contents of GSH, and the activities of SOD and CAT in the studied groups were assessed by specific kits. As illustrated in Fig. 2A–C, increased levels of 4-HNE, MDA, and PC in renal tissues were observed after LPS treatment, when compared to the Control group. On the contrary, the promotive impact of LPS on these lipid peroxidative parameters was inhibited by Rg1, which then was reversed by EX527 (Fig. 2A–C). Consistently, LPS contributed to reduced contents of GSH and decreased activities of SOD and CAT in murine kidneys. Conversely, Rg1 partially offset these changes. Moreover, the impact of Rg1 on the above-mentioned antioxidants in murine kidneys following LPS treatment was abrogated by EX527 (Fig. 2D, E). Collectively, Rg1 prevents renal lipid peroxidation and oxidative stress induced by LPS, which were offset by inhibiting SIRT1 with EX527.

Ginsenoside Rg1 suppresses LPS-induced cell apoptosis in renal tissues by upregulating SIRT1

In this part of the study, we verified the protection afforded by Rg1 against apoptotic process in LPS-induced AKI *in vivo*. TUNEL assays confirmed that the apoptosis of renal cells was increased in mouse kidney after LPS administration (Fig. 3A, B). However, Rg1 impeded cell apoptosis in LPS-treated renal tissues (Fig. 3A, B). In comparison with the LPS+Rg1 group, cell apoptosis in the kidney of LPS + Rg1 + EX527 mice was aggravated (Fig. 3A, B). As Fig. 3C, D showed, reduced anti-apoptotic Bcl-2 protein expression, and elevated protein levels of pro-apoptotic Bax and Cleaved caspase-3 in the kidney were induced by LPS, and Rg1 reversed these changes. On the contrary, EX527 treatment abrogated the effects of Rg1 on the protein levels of these apoptosis-related markers (Fig. 3C, D). To sum up, Rg1 impedes LPS-induced apoptosis in renal tissues, which was counteracted by inhibiting SIRT1 with EX527.

Ginsenoside Rg1 suppresses LPS-induced renal inflammation by upregulating SIRT1

Compared to the Control group, the concentrations of IL-1β, TNF-α, and IL-6 in the kidney homogenates were increased in LPS-induced mice, which was reversed by Rg1; however, this effect of Rg1 was inhibited by EX527 (Fig. 4A, C). Consistently, Rg1 suppressed LPS-mediated increase in the protein levels of IL-1β, TNF-α, and IL-6 in the kidney as measured by western blotting (Fig. 4D). Furthermore, administration of EX527 reversed this protective effect of Rg1 in LPS-treated mice (Fig. 4D). To sum up, Rg1 protects murine kidneys against LPS-evoked inflammation,

Folia Histochem Cytobiol. 2024
DOI: 10.5603/fhc.97140
ISSN 0239-8508, e-ISSN 1897-5631

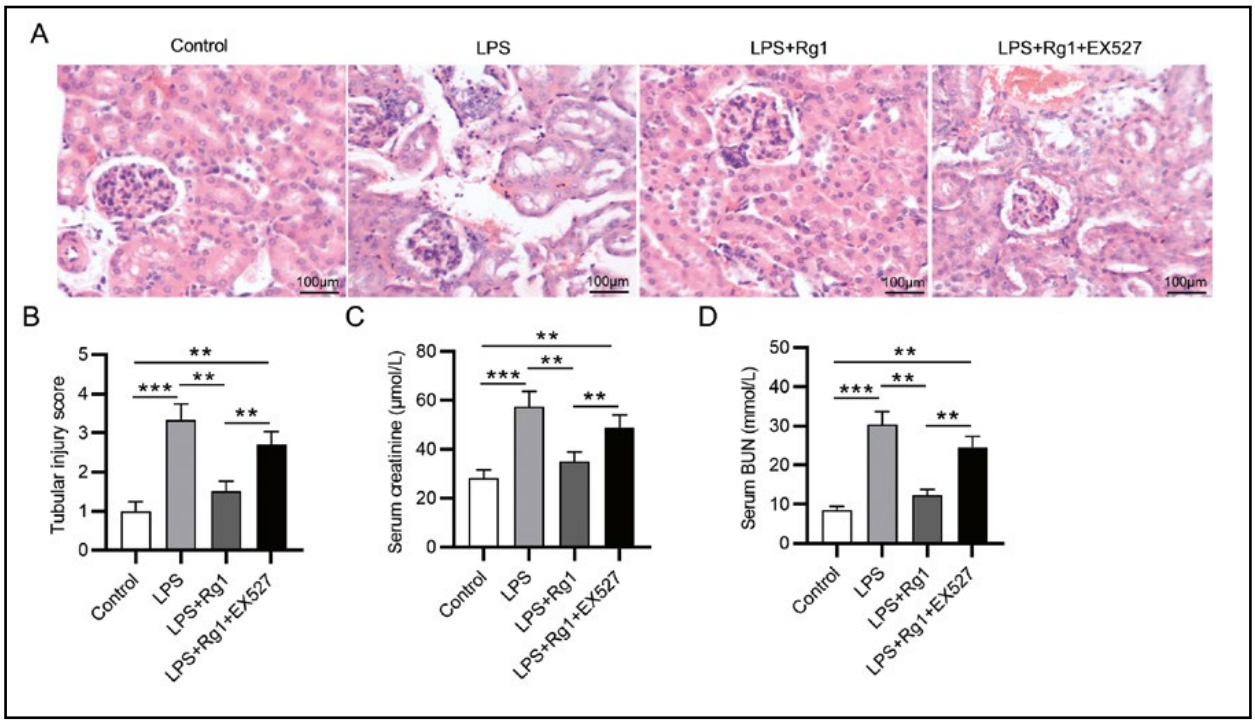

Figure 1. Ginsenoside Rg1 attenuates LPS-induced renal injury by upregulating SIRT1. **A.** HE staining for observing renal histological changes in the Control, LPS, LPS+Rg1, and LPS + Rg1 + EX527 mice groups. Scale bar = 100 μm. **B.** Tubular injury score in the Control, LPS, LPS + Rg1, and LPS + Rg1 + EX527 mice groups was determined as described in Methods. **C, D.** Serum creatinine and BUN levels were measured in the studied mice groups as described in Methods. **P < 0.01, ***P < 0.001.

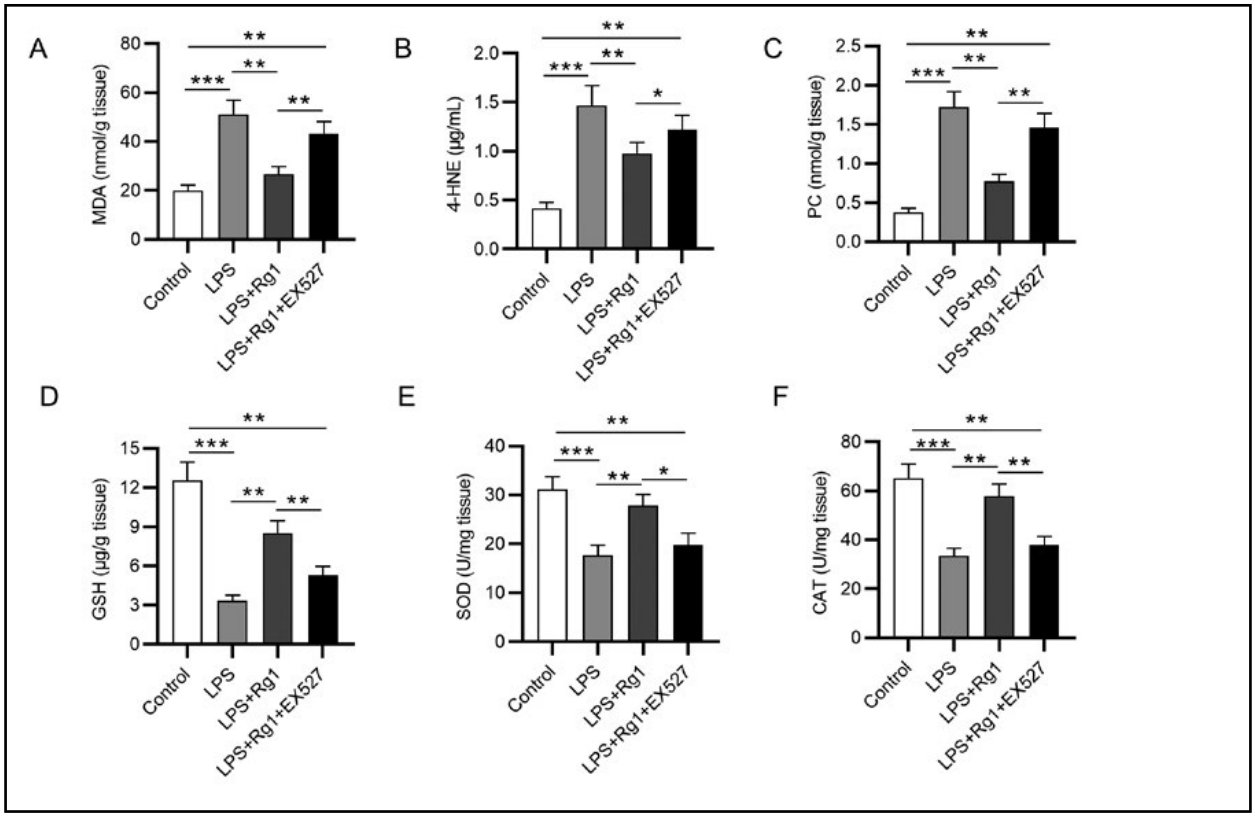

Figure 2. Rg1 inhibits LPS-triggered renal oxidative stress by upregulating SIRT1. Measurement of (**A**) malondialdehyde (MDA), (**B**) 4-hydroxynonenal (4-HNE), (**C**) protein carbonyl groups (PC), and (**D**) GSH contents, (**E**) sodium dismutase (SOD) activities, and (**F**) catalase (CAT) activities in the kidneys of the Control, LPS, LPS + Rg1, and LPS + Rg1 + EX527 mice groups were determined as described in Methods. *P < 0.05, **P < 0.01, ***P < 0.001.

Folia Histochem Cytobiol. 2024
DOI: 10.5603/fhc.97140
ISSN 0239-8508, e-ISSN 1897-5631

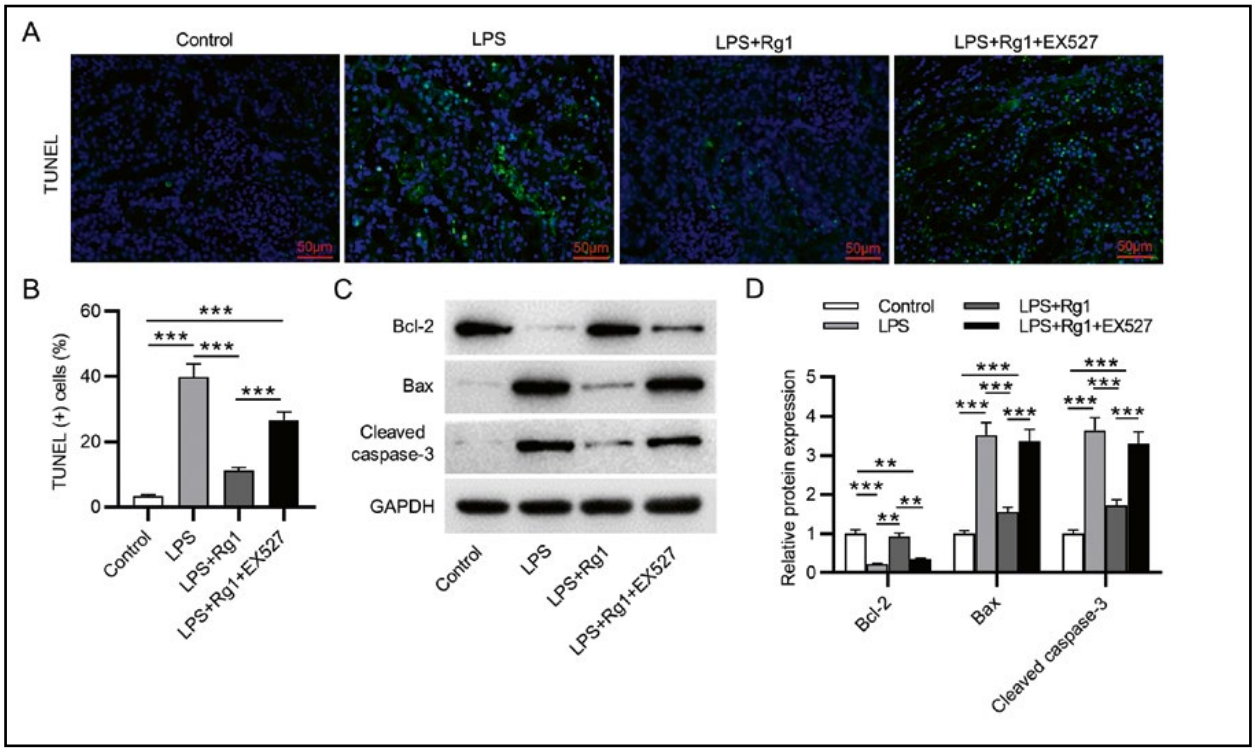

Figure 3. Rg1 suppresses LPS-induced cell apoptosis in renal tissues by upregulating SIRT1. **A, B.** TUNEL assay for evaluating cell apoptosis in the kidneys of the Control, LPS, LPS + Rg1, and LPS + Rg1 + EX527 mice groups. Scale bar = 100 μm. **C, D.** Western blotting was used to assess apoptosis-related marker protein levels in the kidneys of the studied mice groups. * P < 0.05, **P < 0.01, ***P < 0.001.

which was counteracted by the pre-treatment of mice with EX527, a SIRT1 inhibitor.

Ginsenoside Rg1 regulates SIRT1/NF-κB signaling in LPS-induced S-AKI mice

By the use of western blot technique we showed that LPS decreased SIRT1 protein level in the murine kidney and that Rg1 suppressed this effect. However, EX527 pretreatment abolished the protective effect of Rg1 in the kidney of LPS-induced mice (Fig. 5A). Rg1 also restored LPS-mediated reduction in the activity of SIRT1 in the kidney. However, this effect was inhibited by EX527 (Fig. 5B). Additionally, the IκBα protein expression was decreased and the p-NF-κB p65/NF-κB p65 ratio in the kidney was increased after LPS administration. On the contrary, Rg1 upregulated IκBα protein expression and downregulated phosphorylated NF-κB p65 protein expression in the kidney of LPS-treated mice. Compared to the LPS + Rg1 group, the LPS + Rg1 + EX527 group exhibited reduced IκBα protein expression and elevated phosphorylated NF-κB p65 protein expression (Fig. 5C, D). Moreover, we found that the fluorescence intensity of p-NF-κB p65 was enhanced after LPS treatment in the kidney, while this effect was reversed by Rg1 (Fig. 5E). The inhibitory impact on the fluorescence intensity of p-NF-κB p65 exerted by Rg1 was mitigated by EX527 in the kidney of LPS-treated mice (Fig. 5E). Therefore, Rg1 represses LPS-induced activation of NF-κB signaling in LPS-induced AKI mouse model, which was antagonized by inhibiting SIRT1 with EX527.

Discussion

Half of AKI cases in critically ill patients are attributed to sepsis, and S-AKI is related to unacceptable mortality in hospitalization [3]. Emerging reports have validated the efficacy of Chinese medicine herbs in S-AKI, such as honokiol [31], resveratrol [32], and shionone [33]. Rg1 is the main active component of *Panax ginseng* and has many pharmacological properties [34]. In recent years, the protection afforded by Rg1 has been confirmed in sepsis [35] and sepsis-related diseases, including septic acute lung injury [36], septic cardiac dysfunction [37], and septic encephalopathy [38]. Additionally, several studies have demonstrated the beneficial role of Rg1 in many types of experimental models of renal disorders, such as obstructive nephropathy [39] and unilateral ureteral obstruction [40]. Notably, Rg1 has been reported to attenuate chronic renal injury induced by low-dose LPS in mice by reducing ROS generation and renal

DOI: 10.5603/fhc.97140
ISSN 0239-8508, e-ISSN 1897-5631

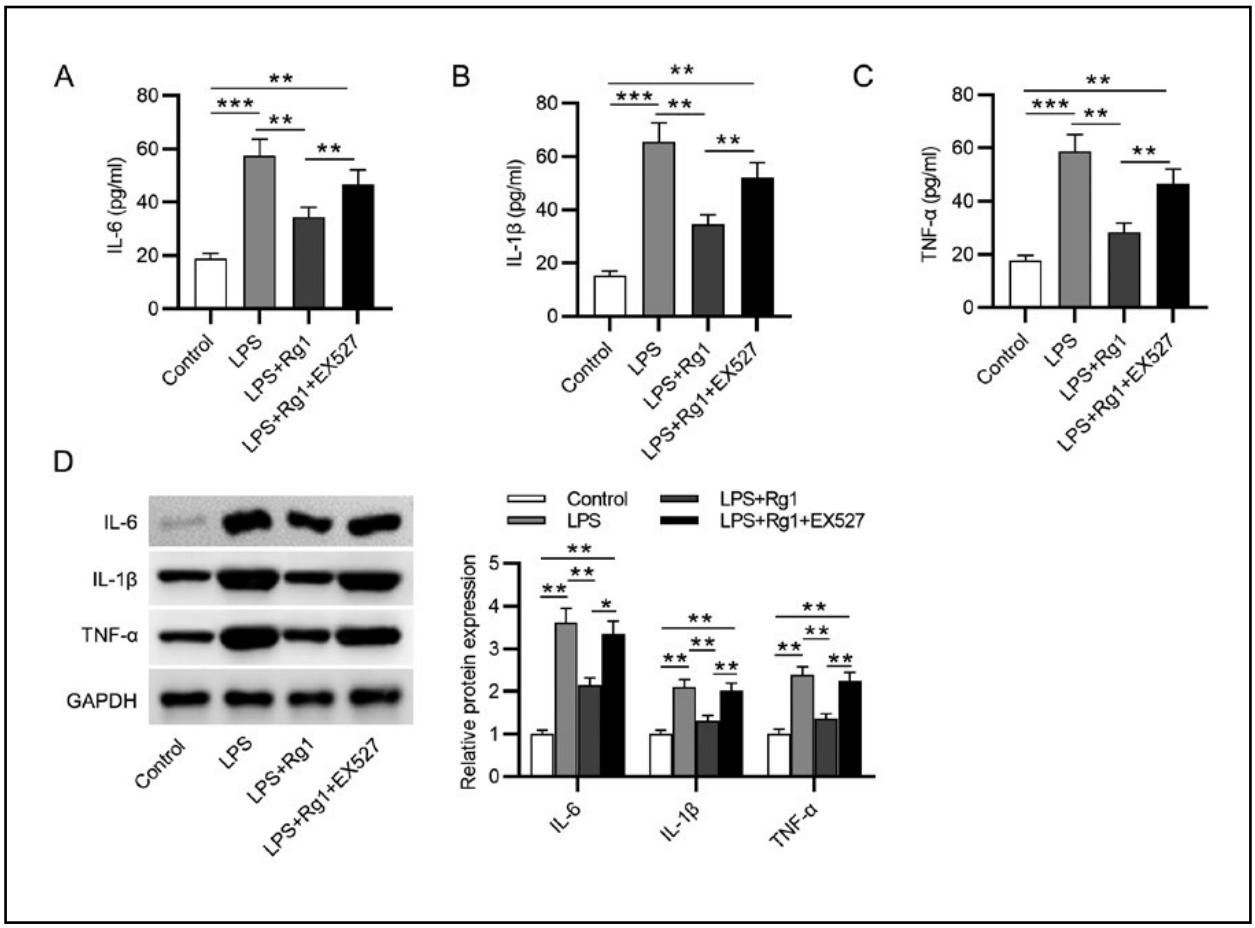

Figure 4. Rg1 suppresses LPS-induced renal inflammation by upregulating SIRT1. **A–C.** ELISA was used to assess proinflammatory cytokines' (IL-6, IL-1β, and TNF-α) concentrations in the kidneys in the Control, LPS, LPS + Rg1, and LPS + Rg1 + EX527 groups. **D.** Western blots demonstrate proinflammatory cytokine protein levels in the kidneys of the studied mice groups. *P < 0.05, **P < 0.01, ***P < 0.001.

fibrosis [41]. Our findings demonstrated that Rg1 exerted anti-inflammatory, anti-apoptotic, and antioxidant effects to ameliorate LPS-induced acute kidney injury by affecting the SIRT1/NF-κB signaling.

Lipopolysaccharide has been extensively utilized to establish the animal models of AKI, which is similar with pathological characteristics to S-AKI in human [42]. In this study, the *in vivo* model of S-AKI was established through the intraperitoneal injection of LPS into mice. Through histological examinations, characteristic morphological features of renal injury, including inflammatory cell accumulation, renal tubular epithelial cell necrosis, glomerular structure damage, and glomerular degeneration in renal cortex, were induced by LPS. However, these renal lesions were ameliorated by Rg1. Serum BUN and creatinine are key indexes that can reflect renal dysfunction [43]. Here, the levels of serum BUN and creatinine were increased after LPS injection, which were restored by Rg1 treatment, suggesting that Rg1 improves renal function. Therefore, Rg1 exerts nephroprotective effects against S-AKI by ameliorating renal dysfunction and histopathological changes. Likewise, the alleviative effects of Rg1 on renal pathological injury and kidney dysfunction have also been validated in a rat model of unilateral ureteral obstruction [44], further confirming the nephroprotective role of Rg1.

Oxidative stress, chronic inflammation, and renal cell apoptosis are important pathogenic factors in the pathophysiology of S-AKI [45–49]. After LPS administration, endogenous antioxidant system is disrupted and ROS are excessively generated, contributing to the pathogenesis of S-AKI [50]. Studies have validated the anti-inflammatory and antioxidative effects of Rg1 in aldosterone-induced renal injury [51] and diabetic nephropathy [52]. In this report, LPS administration reduced the contents of GSH, the activities of SOD and CAT, and increased the contents of lipid peroxidation markers (MDA, 4-HNE and PC) in murine kidneys. However, Rg1 administration reversed these changes induced by LPS. This result suggested the antioxidant effects of Rg1 against LPS-induced AKI. LPS

Folia Histochem Cytobiol. 2024
DOI: 10.5603/fhc.97140
ISSN 0239-8508, e-ISSN 1897-5631

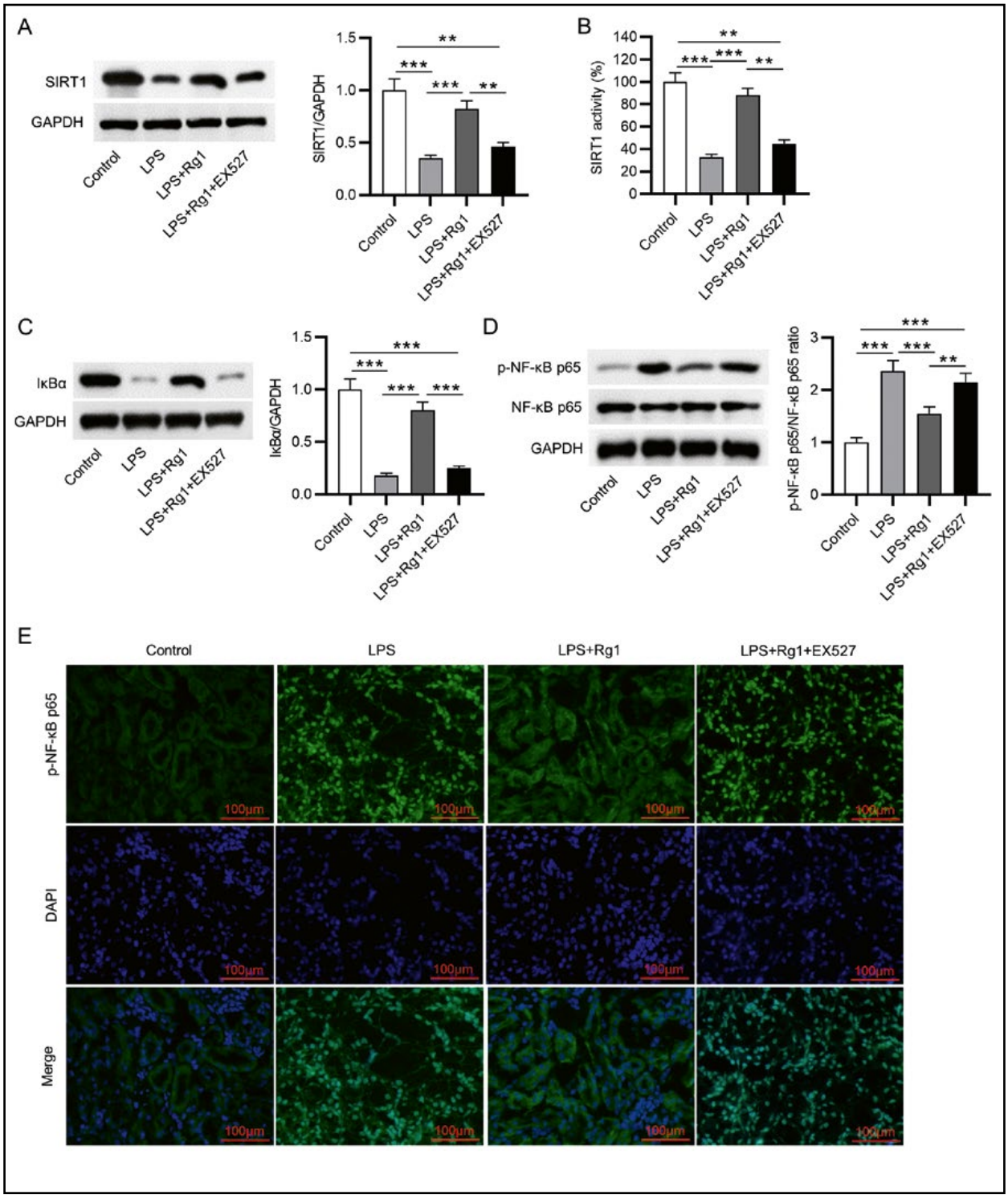

Figure 5. Rg1 regulates SIRT1/NF-κB signaling in LPS-induced S-AKI mice. Western blotting was applied to measure the protein levels of (**A**) sirtuin 1 (SIRT1), (**C**) IκBα, and (**D**) p-NF-κB p65 and NF-κB p65 in the kidneys of the Control, LPS, LPS + Rg1, and LPS + Rg1 + EX527 groups. **B.** SIRT1 activity in the kidneys of the studied mice groups. **E.** Immunofluorescence was used as described in Methods to detect the fluorescence intensity of p-NF-κB p65 in the kidneys of the studied mice groups. Scale bar = 100 μm. **P < 0.01, ***P < 0.001.

challenge also induced the release of proinflammatory cytokines which were found to aggravate renal inflammation in S-AKI [53, 54]. In the current study, LPS administration increased IL-6, IL-1β, and TNF-α levels in kidney homogenates, while this event was neutralized by Rg1. Thus, the protection afforded by Rg1 in S-AKI may be achieved also by its anti-inflammatory effects. Interestingly, it has been demonstrated

DOI: 10.5603/fhc.97140
ISSN 0239-8508, e-ISSN 1897-5631

that Rg1 also attenuates inflammation in a model of septic acute lung injury [36] and cadmium-induced neurotoxicity [55].

Increased renal apoptosis is a hallmark of S-AKI [56–58]. Previously, Rg1 was found to exert anti-apoptotic effects in kidney ischemia/reperfusion [59], septic acute lung injury [60], and chronic cyclosporin A-induced nephropathy [61]. In our study, LPS triggered renal cell apoptosis in mice, which was demonstrated by increased number of TUNEL-positive cells, elevated levels of Bax and Cleaved caspase-3, and reduced levels of Bcl-2 in the kidney after LPS treatment. However, these changes were reversed by Rg1. Overall, we showed that Rg1 protects against LPS-induced S-AKI through its antioxidative, anti-inflammatory, and anti-apoptotic properties.

SIRT1 plays an important role in the regulation of inflammatory and oxidative injury by reducing the production of proinflammatory cytokines and improving antioxidant defenses [62, 63]. Emerging evidence has demonstrated that SIRT1 upregulation inhibits S-AKI progression [64–66]. Previously, Wang *et al.* [23] showed that Rg1 alleviates sepsis-induced pulmonary damage by repressing inflammatory response and endoplasmic reticulum stress in LPS-challenged human pulmonary epithelial cells and cecal ligation and puncture-induced sepsis mouse model *via* the regulation of SIRT1. Here, Rg1 reversed LPS-induced reduction in SIRT1 expression and activity in murine kidneys. Moreover, to validate the protective role of SIRT1 in the LPS-induced S-AKI, EX527, a SIRT1 inhibitor, was used as the pre-treatment to Rg1 administration. In a result, EX527 reversed the protective effects of Rg1 on renal pathological changes, proinflammatory cytokine release, antioxidants' levels and activities, lipid peroxidative parameters, and renal cell apoptosis in LPS-induced S-AKI mice, confirming the protective effects of SIRT1 against S-AKI. Thus, Rg1 may exert its beneficial effects in LPS-induced S-AKI by activating SIRT1.

NF-κB signaling has been involved in the induction of inflammatory responses in various pathological disorders [67]. Once NF-κB pathway is activated, the degradation of IκBα and the phosphorylation of p65 and IκBα occur, leading to synthesis and an accumulation of proinflammatory cytokines [68]. A recent study reports that Rg1 ameliorates inflammation in ulcerative colitis in mice *vi*a the inhibition of NF--κB signaling [69]. Evidence has demonstrated the regulatory role of Rg1 in the modulation of NF-κB signaling in palmitic acid-induced steatosis in HepG2 cells [70]. SIRT1 negatively regulates NF-κB pathway to inhibit inflammation, which has been confirmed in LPS-induced mouse peritoneal macrophages and mouse sepsis models [71, 72]. In this study, decreased IκBα and increased phosphorylated p65 levels in renal tissues were observed after LPS administration, all these changes induced by LPS were reversed by Rg1 suggesting that Rg1 represses LPS-induced activation of the NF-κB signaling. Moreover, EX527 treatment counteracted the effects of Rg1 on NF-κB signaling. These results indicated that Rg1 may exert its inflammatory effects by inhibiting SIRT1-mediated NF-κB signaling in S-AKI mice.

To conclude, our study provided the first evidence about the beneficial role of Rg1 in the murine model of LPS-induced S-AKI. In detail, Rg1 ameliorates kidney injury and reduces renal cell apoptosis, oxidative injury, and inflammation in S-AKI mice by regulating the SIRT1/NF-κB signaling. Thus, Rg1 might be an available and effective therapeutic agent in the treatment of S-AKI in humans. However, the side or adverse effects of Rg1 administration to patients still need further exploration. Additionally, the molecules or other signaling pathways associated with the Rg1's effects in S-AKI deserve further investigation.

Article information and declarations

Data availability statement

The datasets used or analyzed during the current study are available from the corresponding author on reasonable request.

Ethics statement

Experimental protocols were granted approval from the Ethics Committee of the Graduate School of Medicine at Wuhan Hospital of Traditional Chinese Medicine.

Author contributions

Yadan Hu and Chao Xiang were the main designers of this study. Yadan Hu, Chao Xiang, Dong Zhang, Fang Zhou and Dede Zhang performed the experiments and analyzed the data. Yadan Hu, Chao Xiang, Dong Zhang and Dede Zhang drafted the manuscript. All authors read and approved the final manuscript.

Funding

None.

Acknowledgments

The authors appreciate all the participants providing supports for this study.

Conflict of interest

The authors declare that they have no competing interests.

References

1. Uhle F, Lichtenstern C, Brenner T, et al. Pathophysiology of sepsis. Anasthesiol Intensivmed Notfallmed Schmerzther. 2015; 50(2): 114–122, doi: 10.1055/s-0041-100391, indexed in Pubmed: 25723606.
2. Poston JT, Koyner JL. Sepsis associated acute kidney injury. BMJ. 2019; 364: k4891, doi: 10.1136/bmj.k4891, indexed in Pubmed: 30626586.
3. Peerapornratana S, Manrique-Caballero CL, Gómez H, et al. Acute kidney injury from sepsis: current concepts, epidemiology, pathophysiology, prevention and treatment. Kidney Int. 2019; 96(5): 1083–1099, doi: 10.1016/j.kint.2019.05.026, indexed in Pubmed: 31443997.
4. Manrique-Caballero CL, Del Rio-Pertuz G, Gomez H. Sepsis-associated acute kidney injury. Crit Care Clin. 2021; 37(2): 279–301, doi: 10.1016/j.ccc.2020.11.010, indexed in Pubmed: 33752856.
5. Gomez H, Ince C, De Backer D, et al. A unified theory of sepsis-induced acute kidney injury: inflammation, microcirculatory dysfunction, bioenergetics, and the tubular cell adaptation to injury. Shock. 2014; 41(1): 3–11, doi: 10.1097/SHK.0000000000000052, indexed in Pubmed: 24346647.
6. Stasi A, Intini A, Divella C, et al. Emerging role of Lipopolysaccharide binding protein in sepsis-induced acute kidney injury. Nephrol Dial Transplant. 2017; 32(1): 24–31, doi: 10.1093/ndt/gfw250, indexed in Pubmed: 27387474.
7. Wang Z, Wu J, Hu Z, et al. Dexmedetomidine alleviates lipopolysaccharide-induced acute kidney injury by inhibiting p75NTR-Mediated oxidative stress and apoptosis. Oxid Med Cell Longev. 2020; 2020: 5454210, doi: 10.1155/2020/5454210, indexed in Pubmed: 33194004.
8. Yoo JY, Cha DR, Kim B, et al. LPS-Induced acute kidney injury is mediated by Nox4-SH3YL1. Cell Rep. 2020; 33(3): 108245, doi: 10.1016/j.celrep.2020.108245, indexed in Pubmed: 33086058.
9. Huang G, Bao J, Shao X, et al. Inhibiting pannexin-1 alleviates sepsis-induced acute kidney injury via decreasing NLRP3 inflammasome activation and cell apoptosis. Life Sci. 2020; 254: 117791, doi: 10.1016/j.lfs.2020.117791, indexed in Pubmed: 32416166.
10. Chen J, Zhang X, Liu X, et al. Ginsenoside Rg1 promotes cerebral angiogenesis via the PI3K/Akt/mTOR signaling pathway in ischemic mice. Eur J Pharmacol. 2019; 856: 172418, doi: 10.1016/j.ejphar.2019.172418, indexed in Pubmed: 31132356.
11. Zou Y, Tao T, Tian Ye, et al. Ginsenoside Rg1 improves survival in a murine model of polymicrobial sepsis by suppressing the inflammatory response and apoptosis of lymphocytes. J Surg Res. 2013; 183(2): 760–766, doi: 10.1016/j.jss.2013.01.068, indexed in Pubmed: 23478085.
12. Mei X, Feng H, Shao B. Alleviation of sepsis-associated encephalopathy by ginsenoside via inhibition of oxidative stress and cell apoptosis: An experimental study. Pak J Pharm Sci. 2020; 33(6): 2567–2577, indexed in Pubmed: 33867332.
13. Luo M, Yan D, Sun Q, et al. Ginsenoside Rg1 attenuates cardiomyocyte apoptosis and inflammation via the TLR4/NF-kB/NLRP3 pathway. J Cell Biochem. 2020; 121(4): 2994–3004, doi: 10.1002/jcb.29556, indexed in Pubmed: 31709615.
14. Mao N, Tan RZ, Wang SQ, et al. Ginsenoside Rg1 inhibits angiotensin II-induced podocyte autophagy via AMPK/mTOR/PI3K pathway. Cell Biol Int. 2016; 40(8): 917–925, doi: 10.1002/cbin.10634, indexed in Pubmed: 27296076.
15. Guo X, Zhang J, Liu M, et al. Protective effect of ginsenoside Rg1 on attenuating anti-GBM glomerular nephritis by activating NRF2 signalling. Artif Cells Nanomed Biotechnol. 2019; 47(1): 2972–2979, doi: 10.1080/21691401.2019.1640712, indexed in Pubmed: 31322005.
16. Shen X, Dong X, Han Y, et al. Ginsenoside Rg1 ameliorates glomerular fibrosis during kidney aging by inhibiting NOX4 and NLRP3 inflammasome activation in SAMP8 mice. Int Immunopharmacol. 2020 [Epub ahead of print]; 82: 106339, doi: 10.1016/j.intimp.2020.106339, indexed in Pubmed: 32114413.
17. Chen C, Zhou M, Ge Y, et al. SIRT1 and aging related signaling pathways. Mech Ageing Dev. 2020; 187: 111215, doi: 10.1016/j.mad.2020.111215, indexed in Pubmed: 32084459.
18. Wei S, Gao Y, Dai X, et al. SIRT1-mediated HMGB1 deacetylation suppresses sepsis-associated acute kidney injury. Am J Physiol Renal Physiol. 2019; 316(1): F20–F31, doi: 10.1152/ajprenal.00119.2018, indexed in Pubmed: 30379096.
19. Li Lu, Liu X, Li S, et al. Tetrahydrocurcumin protects against sepsis-induced acute kidney injury via the SIRT1 pathway. Ren Fail. 2021; 43(1): 1028–1040, doi: 10.1080/0886022X.2021.1942915, indexed in Pubmed: 34187277.
20. Kauppinen A, Suuronen T, Ojala J, et al. Antagonistic crosstalk between NF-κB and SIRT1 in the regulation of inflammation and metabolic disorders. Cellular Signalling. 2013; 25(10): 1939––1948, doi: 10.1016/j.cellsig.2013.06.007.
21. DiDonato JA, Mercurio F, Karin M. NF-κB and the link between inflammation and cancer. Immunol Rev. 2012; 246(1): 379–400, doi: 10.1111/j.1600-065X.2012.01099.x, indexed in Pubmed: 22435567.
22. Lu S, Zhou S, Chen J, et al. Quercetin nanoparticle ameliorates lipopolysaccharide-triggered renal inflammatory impairment by regulation of sirt1/nf-kb pathway. J Biomed Nanotechnol. 2021; 17(2): 230–241, doi: 10.1166/jbn.2021.3031, indexed in Pubmed: 33785094.
23. Wang QL, Yang L, Peng Y, et al. Ginsenoside Rg1 Regulates SIRT1 to Ameliorate Sepsis-Induced Lung Inflammation and Injury via Inhibiting Endoplasmic Reticulum Stress and Inflammation. Mediators Inflamm. 2019; 2019: 6453296, doi: 10.1155/2019/6453296, indexed in Pubmed: 30918470.
24. Nadeem A, Ahmad SF, Al-Harbi NO, et al. Role of ITK signaling in acute kidney injury in mice: amelioration of acute kidney injury associated clinical parameters and attenuation of inflammatory transcription factor signaling in CD4+ T cells by ITK inhibition. Int Immunopharmacol. 2021; 99: 108028, doi: 10.1016/j.intimp.2021.108028, indexed in Pubmed: 34365077.
25. Wang XY, Li XY, Wu CH, et al. Protectin conjugates in tissue regeneration 1 restores lipopolysaccharide-induced pulmonary endothelial glycocalyx loss via ALX/SIRT1/NF-kappa B axis. Respir Res. 2021; 22(1): 193, doi: 10.1186/s12931-021-01793-x, indexed in Pubmed: 34217286.
26. Li Y, Wang F, Luo Y. Ginsenoside Rg1 protects against sepsis-associated encephalopathy through beclin 1-independent autophagy in mice. J Surg Res. 2017; 207: 181–189, doi: 10.1016/j.jss.2016.08.080, indexed in Pubmed: 27979475.
27. Shen Y, Qiu T, Liu XH, et al. Renal ischemia-reperfusion injury attenuated by splenic ischemic preconditioning. Eur Rev Med Pharmacol Sci. 2018; 22(7): 2134–2142, doi: 10.26355/eurrev_201804_14747, indexed in Pubmed: 29687873.
28. Zhao X, Wang M, Sun Z, et al. MicroRNA-139-5p improves sepsis-induced lung injury by targeting Rho-kinase1. Exp Ther Med. 2021; 22(4): 1059, doi: 10.3892/etm.2021.10493, indexed in Pubmed: 34434273.

Folia Histochem Cytobiol. 2024
DOI: 10.5603/fhc.97140
ISSN 0239-8508, e-ISSN 1897-5631

29. Jensen EC. Quantitative analysis of histological staining and fluorescence using ImageJ. Anat Rec (Hoboken). 2013; 296(3): 378–381, doi: 10.1002/ar.22641, indexed in Pubmed: 23382140.
30. Pan T, Jia P, Chen N, et al. Delayed remote ischemic preconditioning confersrenoprotection against septic acute kidney injury via exosomal miR-21. Theranostics. 2019; 9(2): 405–423, doi: 10.7150/thno.29832, indexed in Pubmed: 30809283.
31. Xia S, Lin H, Liu H, et al. Honokiol attenuates sepsis-associated acute kidney injury via the inhibition of oxidative stress and inflammation. Inflammation. 2019; 42(3): 826–834, doi: 10.1007/s10753-018-0937-x, indexed in Pubmed: 30680694.
32. Wang Y, Feng F, Liu M, et al. Resveratrol ameliorates sepsis-induced acute kidney injury in a pediatric rat model via Nrf2 signaling pathway. Exp Ther Med. 2018; 16(4): 3233–3240, doi: 10.3892/etm.2018.6533, indexed in Pubmed: 30214546.
33. Zhang B, Xue Yi, Zhao J, et al. Shionone attenuates sepsis-induced acute kidney injury by regulating macrophage polarization the ECM1/STAT5 pathway. Front Med (Lausanne). 2021; 8: 796743, doi: 10.3389/fmed.2021.796743, indexed in Pubmed: 35141243.
34. Xu X, Qu Z, Qian H, et al. Ginsenoside Rg1 ameliorates reproductive function injury in C57BL/6J mice induced by di-N-butylphthalate. Environ Toxicol. 2021; 36(5): 789–799, doi: 10.1002/tox.23081, indexed in Pubmed: 33331133.
35. Su F, Xue Y, Wang Y, et al. Protective effect of ginsenosides Rg1 and Re on lipopolysaccharide-induced sepsis by competitive binding to Toll-like receptor 4. Antimicrob Agents Chemother. 2015; 59(9): 5654–5663, doi: 10.1128/AAC.01381-15, indexed in Pubmed: 26149990.
36. Zhang ZB, Xu QP. Experimental study of ginsenoside Rg1 combined with antibiotics in the treatment of acute lung injury in mice with sepsis. Sichuan Da Xue Xue Bao Yi Xue Ban. 2020; 51(3): 371–375, doi: 10.12182/20200560204, indexed in Pubmed: 32543145.
37. Liu Z, Pan H, Zhang Y, et al. Ginsenoside-Rg1 attenuates sepsis-induced cardiac dysfunction by modulating mitochondrial damage via the P2X7 receptor-mediated Akt/GSK-3β signaling pathway. J Biochem Mol Toxicol. 2022; 36(1): e22885, doi: 10.1002/jbt.22885, indexed in Pubmed: 34859534.
38. Chen Y, Chi M, Qiao X, et al. Anti-inflammatory effect of ginsenoside Rg1 on LPS-induced septic encephalopathy and associated mechanism. Curr Neurovasc Res. 2022; 19(1): 38–46, doi: 10.2174/1567202619666220414093130, indexed in Pubmed: 35430992.
39. Li SS, He AL, Deng ZY, et al. Ginsenoside-Rg1 protects against renal fibrosis by regulating the klotho/tTGF-β1/Smad signaling pathway in rats with obstructive nephropathy. Biol Pharm Bull. 2018; 41(4): 585–591, doi: 10.1248/bpb.b17-00934, indexed in Pubmed: 29607931.
40. Xie XS, Yang M, Liu HC, et al. Influence of ginsenoside Rg1, a panaxatriol saponin from Panax notoginseng, on renal fibrosis in rats with unilateral ureteral obstruction. J Zhejiang Univ Sci B. 2008; 9(11): 885–894, doi: 10.1631/jzus.B0820024, indexed in Pubmed: 18988308.
41. Zhang D, Ji P, Sun R, et al. Ginsenoside Rg1 attenuates LPS-induced chronic renal injury by inhibiting NOX4-NLRP3 signaling in mice. Biomed Pharmacother. 2022; 150: 112936, doi: 10.1016/j.biopha.2022.112936, indexed in Pubmed: 35421784.
42. Shimokawa T, Yoneda K, Yamagata M, et al. Yohimbine ameliorates lipopolysaccharide-induced acute kidney injury in rats. Eur J Pharmacol. 2020; 871: 172917, doi: 10.1016/j.ejphar.2020.172917, indexed in Pubmed: 31935395.
43. Qi SS, Zheng HX, Jiang H, et al. Protective effects of chromium picolinate against diabetic-induced renal dysfunction and renal fibrosis in streptozotocin-induced diabetic rats. Biomolecules. 2020; 10(3), doi: 10.3390/biom10030398, indexed in Pubmed: 32143429.
44. Li SS, Ye Jm, Deng Zy, et al. Ginsenoside-Rg1 inhibits endoplasmic reticulum stress-induced apoptosis after unilateral ureteral obstruction in rats. Ren Fail. 2015; 37(5): 890–895, doi: 10.3109/0886022X.2015.1015427, indexed in Pubmed: 25707520.
45. Xu HP, Ma XY, Yang C. Circular RNA TLK1 promotes sepsis-associated acute kidney injury by regulating inflammation and oxidative stress through miR-106a-5p/HMGB1 axis. Front Mol Biosci. 2021; 8: 660269, doi: 10.3389/fmolb.2021.660269, indexed in Pubmed: 34250012.
46. Ow CPC, Trask-Marino A, Betrie AH, et al. Targeting oxidative stress in septic acute kidney injury: from theory to practice. J Clin Med. 2021; 10(17), doi: 10.3390/jcm10173798, indexed in Pubmed: 34501245.
47. Pavlakou P, Liakopoulos V, Eleftheriadis T, et al. Oxidative Stress and Acute Kidney Injury in Critical Illness: Pathophysiologic Mechanisms-Biomarkers-Interventions, and Future Perspectives. Oxid Med Cell Longev. 2017; 2017: 6193694, doi: 10.1155/2017/6193694, indexed in Pubmed: 29104728.
48. Gui Y, Yang Y, Xu D, et al. Schisantherin A attenuates sepsis-induced acute kidney injury by suppressing inflammation via regulating the NRF2 pathway. Life Sci. 2020; 258: 118161, doi: 10.1016/j.lfs.2020.118161, indexed in Pubmed: 32730835.
49. Zhang J, Yue Y, Ma Y. Ameliorates sepsis-induced acute kidney injury in mice by promoting CXCL14. Allergol Immunopathol (Madr). 2022; 50(6): 187–194, doi: 10.15586/aei.v50i6.733, indexed in Pubmed: 36335463.
50. Liu X, Lu J, Liao Y, et al. Dihydroartemisinin attenuates lipopolysaccharide-induced acute kidney injury by inhibiting inflammation and oxidative stress. Biomed Pharmacother. 2019; 117: 109070, doi: 10.1016/j.biopha.2019.109070, indexed in Pubmed: 31176164.
51. Wang Li, Mao N, Tan RZ, et al. Ginsenoside Rg1 reduces aldosterone-induced autophagy via the AMPK/mTOR pathway in NRK-52E cells. Int J Mol Med. 2015; 36(2): 518–526, doi: 10.3892/ijmm.2015.2242, indexed in Pubmed: 26063203.
52. Du Na, Xu Z, Gao M, et al. Combination of Ginsenoside Rg1 and Astragaloside IV reduces oxidative stress and inhibits TGF-β1//Smads signaling cascade on renal fibrosis in rats with diabetic nephropathy. Drug Des Devel Ther. 2018; 12: 3517–3524, doi: 10.2147/DDDT.S171286, indexed in Pubmed: 30425453.
53. Gu L, Liu J, Xu D, et al. Polydatin prevents LPS-induced acute kidney injury through inhibiting inflammatory and oxidative responses. Microb Pathog. 2019; 137: 103688, doi: 10.1016/j.micpath.2019.103688, indexed in Pubmed: 31445125.
54. Wu TJ, Hsieh YJ, Lu CW, et al. Linagliptin protects against endotoxin-induced acute kidney injury in rats by decreasing inflammatory cytokines and reactive oxygen species. Int J Mol Sci. 2021; 22(20), doi: 10.3390/ijms222011190, indexed in Pubmed: 34681847.
55. Ren TT, Yang JY, Wang J, et al. Gisenoside Rg1 attenuates cadmium-induced neurotoxicity in vitro and in vivo by attenuating oxidative stress and inflammation. Inflamm Res. 2021; 70(10-12): 1151–1164, doi: 10.1007/s00011-021-01513-7, indexed in Pubmed: 34661679.
56. Zhan Y, Zhu M, Liu S, et al. MicroRNA93 inhibits the apoptosis and inflammatory response of tubular epithelial cells via the PTEN/AKT/mTOR pathway in acute kidney injury. Mol Med Rep. 2021; 24(3), doi: 10.3892/mmr.2021.12305, indexed in Pubmed: 34296286.
57. Wang Bo, Xu J, Ren Q, et al. Fatty acid-binding protein 4 is a therapeutic target for septic acute kidney injury by regulating inflammatory response and cell apoptosis. Cell Death Dis. 2022; 13(4): 333, doi: 10.1038/s41419-022-04794-w, indexed in Pubmed: 35410456.

58. Plotnikov EY, Brezgunova AA, Pevzner IB, et al. Mechanisms of LPS-induced acute kidney injury in neonatal and adult rats. Antioxidants (Basel). 2018; 7(8), doi: 10.3390/antiox7080105, indexed in Pubmed: 30096767.
59. Zhu MX, Ran B, Feng ZQ, et al. Effects of Rb1 and Rg1 on the expression of Bcl-2, Bax in apoptosis of HK-2 cells induced by the serum of kidney ischemia/reperfusion. Zhongguo Ying Yong Sheng Li Xue Za Zhi. 2009; 25(4): 496–499, indexed in Pubmed: 21158042.
60. Ji QJ, Sun ZR, Yang ZZ, et al. Protective effect of ginsenoside Rg1 on LPS-induced apoptosis of lung epithelial cells. Mol Immunol. 2021; 136(8): 168–174, doi: 10.1016/j.molimm.2018.11.003, indexed in Pubmed: 30471963.
61. Liu QF, Deng ZY, Ye JM, et al. Ginsenoside Rg1 protects chronic cyclosporin a nephropathy from tubular cell apoptosis by inhibiting endoplasmic reticulum stress in rats. Transplant Proc. 2015; 47(2): 566–569, doi: 10.1016/j.transproceed.2014.10.047, indexed in Pubmed: 25769608.
62. Yang Y, Liu Y, Wang Y, et al. The roles of CCR9/CCL25 in inflammation and inflammation-associated diseases. Front Cell Dev Biol. 2021; 9: 686548, doi: 10.3389/fcell.2021.686548, indexed in Pubmed: 34490243.
63. You Y, Liang W. SIRT1 and SIRT6: The role in aging-related diseases. Biochim Biophys Acta Mol Basis Dis. 2023; 1869(7): 166815, doi: 10.1016/j.bbadis.2023.166815, indexed in Pubmed: 37499928.
64. Deng Z, Sun M, Wu J, et al. SIRT1 attenuates sepsis-induced acute kidney injury via Beclin1 deacetylation-mediated autophagy activation. Cell Death Dis. 2021; 12(2): 217, doi: 10.1038/s41419-021-03508-y, indexed in Pubmed: 33637691.
65. Guo J, Wang R, Liu D. Bone marrow-derived mesenchymal stem cells ameliorate sepsis-induced acute kidney injury by promoting mitophagy of renal tubular epithelial cells the sirt1/parkin axis. Front Endocrinol (Lausanne). 2021; 12: 639165, doi: 10.3389/fendo.2021.639165, indexed in Pubmed: 34248837.
66. Liu P, Shi D. Calcitonin gene-related peptide attenuates LPS-induced acute kidney injury by regulating Sirt1. Med Sci Monit. 2020; 26: e923900, doi: 10.12659/MSM.923900, indexed in Pubmed: 32673294.
67. Lawrence T. The nuclear factor NF-kappaB pathway in inflammation. Cold Spring Harb Perspect Biol. 2009; 1(6): a001651, doi: 10.1101/cshperspect.a001651, indexed in Pubmed: 20457564.
68. Oeckinghaus A, Hayden MS, Ghosh S. Crosstalk in NF-κB signaling pathways. Nat Immunol. 2011; 12(8): 695–708, doi: 10.1038/ni.2065, indexed in Pubmed: 21772278.
69. Chen Y, Zhang Q, Sun L, et al. Ginsenoside Rg1 attenuates dextran sodium sulfate-induced ulcerative colitis in mice. Physiol Res. 2023; 72(6): 783–792, doi: 10.33549/physiolres.935182, indexed in Pubmed: 38215064.
70. Xiao Q, Zhang S, Yang C, et al. Ginsenoside Rg1 ameliorates palmitic acid-induced hepatic steatosis and inflammation in HepG2 cells via the AMPK/NF-B pathway. Int J Endocrinol. 2019; 2019: 7514802, doi: 10.1155/2019/7514802, indexed in Pubmed: 31467529.
71. Wu Z, Chen J, Zhao W, et al. Inhibition of miR-181a attenuates sepsis-induced inflammation and apoptosis by activating Nrf2 and inhibiting NF-κB pathways via targeting SIRT1. Kaohsiung J Med Sci. 2021; 37(3): 200–207, doi: 10.1002/kjm2.12310, indexed in Pubmed: 33058411.
72. Yang Y, Liu Y, He X, et al. ING4 alleviated lipopolysaccharide-induced inflammation by regulating the NF-κB pathway via a direct interaction with SIRT1. Immunol Cell Biol. 2020; 98(2): 127–137, doi: 10.1111/imcb.12308, indexed in Pubmed: 31811786.

Submitted: 29 August, 2023
Accepted after reviews: 12 March, 2024
Available as AoP: 2 April, 2024